Annu. Rev. Earth Planet. Sci. 2003. 31:555–77
doi: 10.1146/annurev.earth.31.100901.141246

HOLOCENE EARTHQUAKE RECORDS FROM THE CASCADIA SUBDUCTION ZONE AND NORTHERN SAN ANDREAS FAULT BASED ON PRECISE DATING OF OFFSHORE TURBIDITES

Chris Goldfinger
College of Oceanic and Atmospheric Sciences, Oregon State University, Corvallis, Oregon 97331; email: gold@coas.oregonstate.edu

C. Hans Nelson[1]
Department of Oceanography, Texas A & M University, College Station, Texas 77843; email: hans@ocean.tamu.edu

Joel E. Johnson
College of Oceanic and Atmospheric Sciences, Oregon State University, Corvallis, Oregon 97331; email: jjohnson@coas.oregonstate.edu

The Shipboard Scientific Party

Key Words paleoseismology, submarine, recurrence patterns, submarine landslides, turbid flows

■ **Abstract** We present preliminary evidence for a ∼10,000-year earthquake record from two major fault systems based on sediment cores collected along the continental margins of western North America. New stratigraphic evidence from Cascadia demonstrates that 13 earthquakes ruptured the entire margin from Vancouver Island to at least the California border since the eruption of the Mazama ash 7700 years ago. The 13 events above this prominent stratigraphic marker have an average repeat time of 600 years, and the youngest event ∼300 years ago coincides with the coastal record. We also extend the record of past earthquakes to the base of the Holocene (at least 9800 years ago), during which 18 events correlate along the same region. The sequence of Holocene events in Cascadia appears to contain a repeating pattern of events, a tantalizing first look at what may be the long-term behavior of a major fault system.

The northern California margin cores show a cyclic record of turbidite beds that may represent Holocene earthquakes on the northern segment of the San Andreas Fault. Preliminary results are in reasonably good agreement with onshore paleoseismic data that indicate an age for the penultimate event in the mid-1600s at several sites and the most likely age for the third event of ∼AD 1300.

[1]Now at Institute Andaluz de Ciencias de la Tierra, CSIC, Univeridad de Grenada, Campus de Fuente Nueva s/n, Granada, 18002.

INTRODUCTION

On the evening of January 26, 1700, a tremendous upheaval offshore from Oregon and Washington caused 600–1000 km of the coast to drop up to 1–2-m below sea level. This enormous earthquake along the Cascadia subduction zone also generated a tsunami locally 10–12-m high. The tsunami spread across the Pacific and was observed and noted in historical records along the coast of Japan. No Europeans were there to describe this event in writing, but it is remembered in Native American oral histories. Based on historical and paleoseismic data from the Cascadia coast, we now believe this event was a magnitude (M_w) 9 subduction earthquake. This paper reviews recent progress in illuminating the long-term history of the Cascadia subduction zone, as well as preliminary attempts to find a similar record along the Northern San Andreas Fault.

Recent rapid advances in Global Positioning System (GPS) technology now make it possible to measure crustal strain accumulation at plate boundaries with a high degree of certainty in only a few years. However, real-time strain measurements can only represent a fraction of one strain cycle. Fundamental questions about the regularity of earthquake recurrence rates and of fault segmentation remain unanswered because we rarely have data on a large number of earthquake cycles for any given fault system. Earthquake cycle models (in general) assume that stress buildup is proportional to the time since the last earthquake. This stress reaccumulation and release cycle is the basis for probabilistic forecasts of seismicity. Such forecasts require information about the size of expected events, average rates of recurrence, and times since the last event. Closely related to this is the long-term behavior of individual faults, fault segments, and the interaction of segments and faults. What is most needed to address these issues is data on spatial and temporal earthquake recurrence for more fault systems over longer spans of time than are currently available.

Paleoseismology fills the gap between short-term geodesy and seismology and longer-term geologic data. Fault systems that lie beneath or adjacent to bodies of water are candidates for turbidite paleoseismology, the determination of an earthquake record from the record of submarine landslides. Unlike more typical paleoseismology on land, the technique does not use fault outcrops and must demonstrate that the events in the geologic record are uniquely generated by earthquakes and not some other natural phenomenon. Nevertheless, these problems can be overcome, and the technique can be a powerful tool for deciphering the earthquake history along an active continental margin.

We have been investigating the use of turbidites as paleo-earthquake proxies at the Cascadia subduction zone (Figure 1) and along the northern San Andreas Fault. A growing body of evidence from these and other margin settings suggests that with favorable physiography and sedimentological conditions, turbidites can be used as earthquake proxies with careful spatial and temporal correlations. Turbidite paleoseismology has also been attempted in Puget Sound (Karlin & Abella 1992), Japan (Inouchi et al. 1996), the Mediterranean

(Anastasakis & Piper 1991, Kastens 1984, Nelson et al. 1995a), the Dead Sea (Niemi & Ben-Avraham 1994), northern California (Field 1984), a Swiss lake (Schnelmann et al., 2002), and even the Arctic Ocean (Grantz et al. 1996), and it is a technique that is evolving into a precise tool for seismotectonics.

USE OF TURBIDITES AS A PALEO-EARTHQUAKE PROXY

Since the classic study of Heezen & Ewing (1952) of the 1929 Grand Banks earthquake and resulting turbidity current, earthquakes have been known to be a leading turbidity current trigger. Yet, their use as a paleoseismic tool is hampered by the numerous other possible triggers. Adams (1990) suggested four plausible mechanisms for turbid flow generation: (*a*) storm wave loading, (*b*) great earthquakes, (*c*) tsunamis, and (*d*) sediment loading. To these we add (*e*) crustal earthquakes; (*f*) slab earthquakes; (*g*) aseismic accretionary wedge slip; (*h*) hyperpycnal flow, when the surge of storm waters directly from rivers into the canyon heads may also trigger turbid flows; and (*i*) gas hydrate destabilization. All of these mechanisms may trigger individual submarine slides and/or turbid flow events, but how can earthquake-triggered events be distinguished from other events?

Numerous investigators have attempted to distinguish seismically generated turbidites from storm, tsunami, and other deposits. Nakajima & Kanai (2000) and Shiki et al. (2000) argue that seismo-turbidites can in some cases be distinguished sedimentologically. They observe that known seismically derived turbidites in the Japan Sea and Lake Biwa are distinguished by wide areal extent, multiple coarse fraction pulses, variable provenance (derived from multiple or line sources), and greater depositional volume than storm-generated events. These investigators observe that known seismo-turbidites caused multiple slump events in many parts of a canyon system, generating multiple pulses in an amalgamated turbidity current, some of which sampled different lithologies that are separable in the turbidite deposit. The seismo-turbidites are complex, with reverse grading, cutouts, and multiple pulses. Gorsline et al. (2000) make similar observations regarding areal extent and volume of seismo-turbidites for the Santa Monica and Alfonso Basins of the California borderland and the Gulf of California, respectively. In general, these investigators observe that known storm sediment surges are thinner, finer grained, and have simple normally graded Bouma sequences.

Although a number of global, regional, or local criteria have been proposed to distinguish between turbidite triggers, most of these are at present poorly developed. A more reliable criterion, at least in cases where the earthquake source is large, and the rupture spans multiple submarine drainage systems, is synchronicity. Synchronicity of turbid flows in multiple drainage systems can be demonstrated by stratigraphic analysis showing that flows from separate systems coalesced at confluences and, to a lesser degree, by the long-term pattern of events in widely separated systems that would require coincidence beyond credibility. If demonstrated, synchronicity of event records over wide regions and spanning long time intervals effectively eliminates most, and sometimes all, nonearthquake triggers.

CASCADIA PALEOSEISMIC HISTORY

The past occurrence of great earthquakes in Cascadia is now well established by both the coastal record of marsh burials and tsunamis (e.g., Nelson et al. 1995b, Atwater & Hemphill-Haley 1997, Kelsey et al. 2002) and more recently the turbidite event paleoseismic record. Consequently, attention has turned to magnitude, recurrence intervals, and segmentation of the margin. Rupture of the entire margin, or segments of it, should leave distinctly different stratigraphic records in both the coastal marshes and the offshore channels that contain the turbidite record. The turbidite event stratigraphy shows a clear record for the northern ~600 km of the Cascadia Basin, the entire length of the subduction zone offshore from Washington and Oregon has ruptured 18 times in great earthquakes during the past ~9800 years. In addition, smaller localized events that did not trigger turbidites may have occurred.

THE COASTAL RECORD

The most extensive paleoseismic record of subduction events on land is found in buried marshes and tsunami runup or washover deposits of thin sand layers with marine diatoms that are interbedded within estuarine or lake muds (Atwater 1992, Atwater & Hempill-Haley 1997, Nelson et al. 1995, Hemphill-Haley 1995, Hutchinson et al. 2000, Kelsey et al. 2002, Nelson et al. 2000). Buried marshes are the result of repeated downwarping of the coast during major subduction earthquakes, in response to release of crustal flexure that was stored between earthquakes. The stratigraphic record reveals these repeated cycles of uplift and subsidence for each earthquake cycle through remains of high- and low-marsh plants. The tsunami deposits are found in individual, up-river estuaries, or in low-lying freshwater lakes near sea level. These records show the repeated rapid submergence of the land followed by a tsunami, which is best explained by a subduction earthquake.

The length and quality of the sedimentary records of past subduction zone earthquakes varies along the Cascadia coast. A 3500-year record of tsunami events is encountered in Willapa Bay, Washington (Atwater & Hempill-Haley 1997). A 7300-year record is under investigation in Bradley Lake, Oregon (Nelson et al. 2000, Ollerhead et al. 2001). A 5500-year record is also being studied in Sixes River estuary (Kelsey et al. 1998, 2002). The recurrence interval of the Willapa Bay tsunami events is as much as 990 years or as little as 140 years (Atwater & Hempill-Haley 1997). A total of 17 tsunami events have been defined in the Bradley Lake record, where the maximum (900 years) and minimum (100 years) recurrence times are similar to those found in Willapa Bay (Hempill-Haley et al. 2000). The Sixes River record of 11 events in 5500 years is found near the Bradley Lake record and also exhibits a wide variance in time between subduction zone earthquake events from as little as 70 years to as much as 900 years. (Kelsey et al. 1998, 2002). In addition to the similar range in time between events in these

long-term coastal records, ~100 to ~1000 years, the average recurrence interval between events is quite close for the Willapa and Sixes estuaries (500–540 years). It is slightly less for Bradley Lake (440 years) (Kelsey et al. 1998, 2002; Nelson et al. 2000). Kelsey et al. (1998, 2002) find that the Willapa and Sixes estuary records of paleoseismic events are comparable for 2400 to 3500 years BP (before present, by convention reported as before 1950) differ between 2400 to 800 years BP, and both show the 1700 AD event (Jacoby et al. 1997, Yamaguchi et al. 1997). The Willapa and Sixes estuary records have multiple soils buried by estuary muds and provide evidence of co-seismic subsidence, incursion of tsunami sands with marine diatoms over the wetland soil surface, and some associated liquefaction features (Atwater & Hemphill-Haley 1997; Kelsey et al. 1998, 2002). The Bradley Lake record is based only on tsunami deposited sands, exhibits a relatively greater number of events per unit time than the estuary records, and has 12 events requiring a tsunami inundation of >5.5 m.

The most abundant high-precision data are available for the most recent subsidence event, radiocarbon ages, which bracket the few decades around AD 1700. Dendrochronology of western red cedar in Washington and other northern-Oregon estuaries show that death occurred between August 1699 and May 1700 (Jacoby et al. 1997, Yamaguchi et al. 1997), and more imprecise ages also bracket this span. The age of this event is supported by evidence of a far-field tsunami in Japan on January 26, AD 1700, which has been attributed to a subduction earthquake on the Cascadia Subduction Zone (Satake et al. 1996). The ~300-year event is widespread, with evidence found from northern California to Vancouver Island. For older events, error bars for numerical ages are significantly larger and the difficulty in identifying anomalous local subsidence events increases.

Although the coastal record has established the existence of a geologic record of large subduction earthquakes, the question of long-term recurrence patterns and determining whether these ruptures affected the entire plate boundary or separate segments remains elusive. This is because, with the inherent imprecision of radiocarbon dates, separate events spaced a few hours to years apart cannot be distinguished. Such ruptures in fact do occur in nature and are the norm in the Nankai subduction zone (Sugiyama 1994), leaving some degree of uncertainty in the Cascadia record.

TURBIDITE CORRELATION AND DATING METHODS

Before reviewing the turbidite records from Cascadia and the San Andreas plate margins, we discuss methods common to both investigations.

Channel Pathway Analysis

In order to avoid biasing by events such as local slumping or deformation of the channel, we analyze swath bathymetric data in all channel systems of the margin to determine whether they have been influenced by such events. Turbidity currents

result from slumps, mostly of unconsolidated material, in the upper reaches of canyons, but the main concern here is large slumps of older blocky material that may attenuate or deflect turbidity currents that might otherwise travel to core sites on the abyssal plain. Another possible influence on the sedimentary record is folding and faulting. Griggs & Kulm (1970) showed that major turbidity currents are up to 100-m high and 17-km wide in the Cascadia Basin, for example. Thus, faulting and folding at reasonable slip rates, and even moderate slumping, are perhaps unlikely sources of disruption of channel flow.

Core Siting

We try to sample each system both down channel and across major channels in order to capture a complete event record and test for sensitivity in both directions. In our Cascadia work, we found that surface morphology in the channels was a critical factor in determining exact sample location. In a gross sense, distance from the source controls grain size. In detail, we found that the turbidite record was very robust and best preserved in thalwegs (modern channel center), on point bars, in the lee of point bars, and on low terraces above the thalweg. The quality of the record and our ability to capture the Holocene interval was, however, sensitive to local conditions. After some trial and error, we found that sampling in the lee of point bars was a good strategy in proximal locations. These locations included the complete record, did not include very coarse material, and tended to have a somewhat expanded record, which increases dating precision by reducing the sample interval needed to get enough forams for ^{14}C dating. In more distal localities, we sampled local sediment pools to find an expanded record in areas with lower sedimentation rates. In any given setting, some trial and error is required to choose sites that offer optimal conditions, which include an expanded record, and a Holocene section that can be cored with existing gear. Backscatter data from sidescan or multibeam systems, showing the strength of sonar returns from the seafloor, were used to reveal depositional patterns, i.e., to distinguish between active sand channels and muddy levees.

Age Control

We use accelerator mass spectrometry (AMS) radiocarbon dating of planktonic microfossils, foraminifera (forams), as our principal method of age determination. AMS ages are determined from the hemipelagic sediments that underlie each turbidite sequence. We avoid benthic forams as they may be reworked and give erratic ages (M. Kashgarian, personal communication, 2000). Our approach is to collect samples from the youngest hemipelagic interval between events to date the overlying event. Though there may be some erosion of this interval, thus biasing events to slightly older ages, we use more distal cores, which are less likely to have basal erosion for primary dating, and inspect the bases visually for evidence of erosion. Previous work has shown that in mid to distal parts of the Cascadia

channel systems, there is little evidence of erosive turbidite emplacement. Although bioturbation can blur the age of the upper 10 cm beneath the surface, there is some evidence that large grains such as forams are not moved vertically within the sediment as much as the sediment is bioturbated, reducing this problem somewhat (Thomson & Weaver 1994). The samples are examined for organic matter and mica, which is characteristic of turbidite tails (the fine-grained sediment in the waning phase of a turbid flow) in this area. The hemipelagic fraction is also distinguished by greater bioturbation (e.g., Nelson et al. 1968, Griggs et al. 1969).

We sieve the hemipelagic sediment below the base of the turbidite and above any underlying turbidite tail to obtain the sand fraction (>0.062 mm) and carefully hand-pick planktonic forams from the minimum interval needed (1–4 cm) to acquire enough forams for an AMS age, $\sim$1.6 milligrams of carbon. This usually requires 600–800 individual foraminifera. Raw AMS radiocarbon ages are reservoir corrected and converted to calendar years by the method of Stuvier & Braziunas (1993). Though there may be a time-varying surface reservoir age (Southon et al. 1990), this has not yet been demonstrated. We are also fortunate to have a ubiquitious ash datum in Cascadia, in the form of the Mazama ash, which is found in all major channel systems. The ash was deposited by the first turbidite following the cataclysmic eruption of Mt. Mazama in southern Oregon 7627 $\pm$ 150 cal yr BP (Zdanowicz et al. 1999). In the Cascadia channel, our AMS intercept age for the youngest event is 304 years BP for the known 1700 Cascadia event. Additionally, the average age (six ^{14}C ages) of the first post-Mazama turbidite events is 7483 $\pm$ 150 BP, within $\sim$150 years of the Mt. Mazama eruption. Both these ages indicate the reservoir corrections are approximately correct.

Event Correlation and Recurrence Intervals

We address the mean interval between turbidite events and variability of this mean by two semi-independent methods: (*a*) directly dating the events and (*b*) accurate determination of the thickness of the hemipelagic sediment interval between turbidite events in selected new cores. This requires distinguishing the end of the turbidite "tail" from the overlying very similar hepeagic sediment. This is done with detailed analysis of coarse fraction constituents (the turbidite tails tend to include micas not present in the hemipelagic sediment) and X-ray images that reveal subtle depositional features. We analyzed all cores using the OSU Geotek multisensor system (MST), which collects gamma density, P-wave velocity, and magnetic susceptibility along the length of each core. In order to establish a complete chronology at a given site, correlation between the piston and trigger cores, box cores, and sometimes multiple cores at the same site is performed. This is because the tops of cores are sometimes lost (most common with piston cores), and separation of core segments may also occur in the piston core. Correlation between multiple cores aided by the MST data is essential in these cases.

THE CASCADIA TURBIDITE RECORD

Cascadia Seismotectonic Setting

The Cascadia subduction zone is formed by the subduction of the oceanic Juan de Fuca and Gorda plates beneath the North American Plate off the coast of northern California, Oregon, Washington, and Vancouver Island (Figure 1). The convergence rate is 40 mm/year directed ~060° at the latitude of Seattle (DeMets & Dixon 1999). Juan de Fuca–North American convergence is oblique, with obliquity increasing southward along the margin. The submarine forearc widens from 60 km off southern Oregon to 150 km off the northern Olympic Peninsula of Washington, where the thick Pleistocene Astoria and Nitinat Fans are presently being accreted to the margin (Figure 1).

The active accretionary thrust faults of the lower slope are characterized by mostly seaward-vergent thrusts on the Oregon margin from 42° to 44°55′ N and north of 48°08′ N off Vancouver Island and by landward-vergent thrusts between 44°55′ and 48°08′ N, on the northern Oregon and Washington margins. The landward-vergent province of the northern Oregon and Washington lower slope may be related to subduction of rapidly deposited and overpressured sediment from the Nitinat and Astoria submarine fans (Seely 1977, MacKay 1992). Off Washington and northern Oregon, the broad accretionary prism is characterized by low wedge taper and widely spaced landward vergent accretionary thrusts and folds (which offscrape virtually all of the incoming sedimentary section). Sparse age data suggest that this prism is Quaternary in age and is building westward at a rate close to the orthogonal component of plate convergence (Westbrook 1994, Goldfinger et al. 1996). This young wedge abuts a steep slope break that separates it from the continental shelf. Much of onshore western Oregon, Washington, and the continental shelf of Oregon is underlain by a basement of Paleocene to middle Eocene oceanic basalt with interbedded sediments, known as the Crescent or Siletzia terrane.

Following the discovery of the first buried marsh sequences on land, Adams (1990) assessed the possibility that turbidites in channels of the Cascadia Basin contained a record of great earthquakes along the Cascadia margin. He examined core logs for the Cascadia Basin channels and determined that many of them had between 13 and 19 turbidites overlying the Mazama ash datum. In particular, he found that three cores along the length of the Cascadia channel contain 13 turbidites and argued that these 13 turbidites correlate along the channel. Adams observed that cores from Juan de Fuca Canyon, and below the confluence of Willapa, Grays, and Quinault Canyons, contain 14–16 turbidites above the Mazama ash. The correlative turbidites in the Cascadia channel lie downstream of the confluence of these channels. If these events had been independently triggered events with more than a few hours separation in time, the channels below the confluence should contain from 26–31 turbidites, not 13 as observed. This simple observation demonstrates synchronous triggering of turbidite events in tributaries, the headwaters of which are separated by 50–150 km (Figure 1*B*). Similar inferences about regionally

triggered synchronous turbidites in separate channels are reported in Pilkey (1988). The extra turbidites in the upstream channels may be the result of smaller events. Adams' work inspired our effort to test this hypothesis by expanding the spatial and temporal record and establishing a precise chronology of events with AMS ages.

In July 1999, we collected 44 (4″ diameter) piston cores, 44 companion trigger cores (also 4″), and 8 box cores in every major canyon/channel system from the northern limit of the Cascadia subduction zone near the Nootka Fault to Cape Mendocino at its southern terminus (Figure 1) (Goldfinger et al. 1999, Nelson & Goldfinger 1999). We found that 13 post-Mazama events are found along 600 km of the margin in the Juan de Fuca [Figures 2 and 3], Cascadia, Willapa, Grays, Astoria, and Rogue Canyon/Channel systems (Figure 1). Though the Holocene-Pleistocene boundary is a bit less certain, we also find a consistent record of 18 Holocene events in Juan de Fuca, Cascadia, and Rogue channels, extending this record to ∼10,000 years. In existing cores, we originally found only 3 post-Mazama events in the middle and lower Astoria Channel, which appeared to contradict Adams' (1990) hypothesis for 13 events. This led us to believe that there might be a separate central segment in the Cascadia Subduction Zone with an independent earthquake record. In new 1999 cores, we find a progressive loss of turbidites, from 13 to 10 to 7 to 6 to 5 events, at each successive downstream channel splay in the upper Astoria Fan. This down-channel loss of events resulting in only

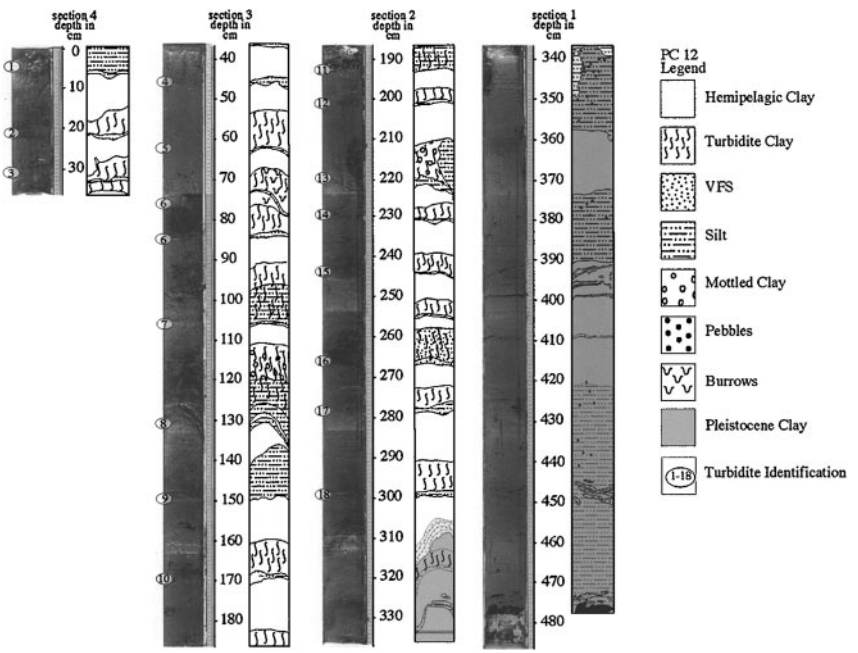

Figure 3 Summary core logs and digital photographs of all sections of Juan de Fuca core 12PC. Turbidites event numbers shown on left side of core.

three events in the mid-lower Astoria Channel explains the previous contradiction and shows that distributary fan systems are poor recorders of the turbidite record as a whole and that there is no separate central segment of the Cascadia Subduction Zone.

Adams (1990) presented convincing evidence that 13 post-Mazama turbidites in separate canyon systems 150-km apart must correlate before they merge into the Cascadia channel system off of Oregon and Washington. We found additional support for this argument in the presence of an identical number of turbidites in other Cascadia Basin channels. Presently this circumstantial argument for correlation rests on the lengthy and consistent record we have collected because there are no other channel confluences to use for additional synchronicity tests. Thus, we cannot rule out the possibility that the northern channels that do converge monitor a single fault segment, whereas other segments rupture separately but with an identical temporal pattern of 18 events in 9800 years.

We can make a few observations regarding other possible triggers and their specific applicability to Cascadia. Storm-wave loading is a reasonable mechanism for triggering of turbid flows but is an unlikely trigger in Cascadia. On the Oregon and Washington margins, although deep-water storm waves are large, the canyon heads where sediment accumulation occurs are at water depths of 150–300 m. These depths are at or below the maximum possible for disturbance by storms with historical maximum significant wave heights of ~20 m, though rare mega storms cannot be ruled out. Tsunamis from distant sources may also act as a regional trigger; however, the tsunami resulting from the 1964 Alaska M_w 9.0 event did not trigger a turbid flow event observed in any of the cores, although it did serious damage along the Pacific coast (Adams 1990).

Crustal or slab earthquakes could also trigger flows that would be recorded in our cores. To investigate this possibility, we resampled the location of a 1986 box core in the Mendocino channel, where the uppermost event is suspected to be the 1906 San Andreas earthquake. Subsequent to the 1986 core, the M_w 7.2 Petrolia earthquake occurred in 1992, either on the plate interface or lowermost accretionary wedge landward of this site (Oppenheimer et al. 1993). Despite the epicentral distance of only a few kilometers from the canyon head, there was no surface sand in the 1999 box core or in other southern Cascadia channel locations. At least for this event, an M_w 7.2 earthquake was not sufficient to trigger a turbid flow, or, alternatively, insufficient sediment was present. Conversely, the Loma Prieta earthquake apparently did trigger some type of turbid flow in Monterey Canyon at a greater epicentral distance (Garfield et al. 1994). We suspect, however, that empirical arguments about triggering magnitudes are of little value and that the many unknowns in play probably make triggering magnitude very site specific.

Hyperpycnal flow, the surge of storm waters directly from rivers into the canyon heads, may also trigger turbid flows (Normark & Piper 1991). In Cascadia, with the exception of the southern Gorda segment, the canyon heads are separated from river mouths by a wide continental shelf during high stands of sea level (Figure 1). The plume from the Columbia River, for example, enters the ocean and, in the

winter storm months when most sediment transport occurs, is driven northward by the Davidson current. Thus, Columbia River sediments mostly do not reach the head of Astoria Canyon. Instead, the sediments are widely distributed on the Washington shelf, and thus the canyon heads are buffered from direct input from the rivers (Sternberg 1986).

South from the Rogue Canyon, the turbidite-event frequency for the northern Gorda-Plate region appears to be the same as for the Cascadia Basin; however, for the southern Gorda area the events are much more frequent. AMS ages indicate that the average turbidite recurrence interval of 133, 75, and 34 years, respectively, for the Trinidad, Eel, and Mendocino channels increases progressively toward the Mendocino triple junction.

The number of possible earthquake triggers also increases progressively toward the triple junction; although, so does the potential for sedimentological triggering. Three earthquakes ranging from 6.9 to 7.4 have occurred in the past 21 years in the triple junction area. However, the thick top layer of hemipelagic sediment (10–14 cm) in the Mendocino Channel is 50 to 70 years old, showing that earthquakes up to 7.4 magnitude have not triggered turbid flow events.

Unlike the other Cascadia systems, both Eel and Mendocino canyon heads erode close to the shoreline, where the canyon heads may intersect littoral drift sediment and also bring them close to river mouths, and where multiple mechanisms may funnel sediments down-canyon without an earthquake trigger. Given the probable mix of interplate, intraplate, and sedimentological events in the southern Gorda region, we are as yet unable to make inferences about the earthquake record in this area.

CASCADIA EARTHQUAKE RECURRENCE INTERVAL DATA INFERRED FROM THE TURBIDITE RECORD

We have plotted the turbidite event age versus recurrence interval for the reliable intervals available as of this writing (Figure 4). The plot includes the best of our "key" cores thus far, PC 12 from Juan De Fuca Canyon (Figures 2 & 3). This is the first of our cores to have all the turbidite events dated down to event 21 (T19 is not included due to age reversal for that event). The 2 sigma error range, shown for individual ages in Figure 2, is not shown on the recurrence plot for simplicity. The plot also includes partial records for the Cascadia and the Rogue systems, for which complete AMS age results are not yet available. We plot recurrence period versus time because comparing cores using the pattern of recurrence rather than the raw ages allows an independent, qualitative look at the pattern. The raw ages have not yet been corrected for sedimentation rate, possible basal erosion, compaction, and tuning of the ^{14}C reservoir correction, and thus direct comparisons are of uncertain value. Each interval is arbitrarily plotted at the younger event age that delimits the interval. Where an event is defined by multiple ages due to multiple intercepts on the ^{14}C calibration curve, we use the median age if there is no statistical preference.

The average post-Mazama recurrence time based on the average of 5 ages (one outlier was discarded) is ~600 years, with the shortest interval being 215 years and the longest being 1488 years. The mean recurrence time based on a tight cluster of three ages for event T18 is ~564 years, which is the Holocene average. The partial Rogue and Cascadia records show a possible pattern correlation with the complete Juan De Fuca record for the overlapping events. One difference is a longer interval between T8 and T9 in the Cascadia core. The Cascadia channel is a distal system, and the Juan de Fuca is more proximal, suggesting an explanation of possible basal erosion in the Juan de Fuca core below T8, which would cause the reported age to be too old (see discussion below).

With a single complete but uncorrected record, the patterns may (or may not) be robust, but there may be a repeating pattern of a long interval, followed by two shorter intervals. Over the past ~7500 years, the pattern appears to have repeated three times, with the most recent AD 1700 event being the third of three events following a long interval of 800–1000 years. This long interval is one that is also recognized in many of the coastal records and may serve as an anchor point between the offshore and onshore records.

Although it is tempting to expound about earthquake clustering and long-term fault behavior, we emphasize here that the analysis shown in Figure 4 is incomplete, and confirmation of this pattern will require age data from the other key cores that is not yet available. We are encouraged that despite occasional reversed ages and other problems inherent in paleoseismology, the extensive turbidite event record in the Cascadia Basin will overcome these problems and, using pattern matching and correlation, will provide a robust long-term paleoseismic history.

PRELIMINARY INVESTIGATION OF TURBIDITE SEQUENCES ALONG THE NORTHERN CALIFORNIA MARGIN

Following on the successful Cascadia effort, we are beginning an investigation of the Holocene rupture history of the northern San Andreas Fault using similar methods. The San Andreas system offers the possibility of developing a long-term earthquake chronology and also of investigating possible fault interactions with the Cascadia Subduction Zone. The plan includes collection of a spatially extensive set of new piston cores in channel systems draining the adjacent continental margin from south of San Francisco to the Mendocino triple junction. This work will utilize a number of "key" cores to develop the Holocene event record in all channel systems draining northern California. Fortunately, we already have one (actually two) of these key cores, collected in Noyo Channel as a control core for the Cascadia project (Figures 5 and 6). We are presently using these two piston cores, as well as box cores, to develop an event history for the northern end of the San Andreas system.

The physiography of the margin is ideal for this investigation. The northern San Andreas Fault has a single main fault strand, and few other regional or

local seismic triggers are available. The margin channels are numerous and offer excellent spatial sampling of the Holocene record along this important fault system. The northern San Andreas Fault offers an excellent opportunity to investigate the long-term history of a relatively simple fault system and relate that history to the current controversy over characteristic versus stress-triggering models of earthquake behavior.

NORTHERN SAN ANDREAS SEISMOTECTONIC SETTING

The San Andreas Fault is probably the best-known transform system in the world. West of the Sierra Nevada block, three main fault systems accommodate ~75% of the Pacific-North America plate motion over a 100-km-wide zone (Argus & Gordon 1991). The remainder is carried by the eastern California shear zone (Argus & Gordon 1991, Sauber et al. 1994). The northern San Andreas Fault is the main system, accommodating approximately 25 mm/year of the ~34 mm/year distributed across western California. Most of the remainder is taken up on the parallel Hayward-Rogers Creek system and the slightly divergent Calaveras Fault system further to the east. South of San Francisco, the transform system becomes more complex and includes the offshore San Gregorio Fault, which joins the northern San Andreas Fault at Olema, just north of San Francisco [Figure 7 and Figure 8]. Between San Francisco and Cape Mendocino, the main strand of the San Andreas Fault is a relatively simple system with most strain localized on the main strand. Seismicity offshore is virtually nil, with the exception of the Mendocino triple junction region. Since the 1906 rupture, the main San Andreas Fault has been nearly aseismic, with only a few small events near Point Arena (Figure 7).

The San Andreas system has been intensely studied on land and has been divided into segments based on its historical record of earthquake behavior. The northern segment ruptured in the 1906 M_w 7.8 earthquake, and rupture extended north from at least San Francisco to Shelter Cove near Point Delgada (Lawson 1908) (Figure 8). Some debate exists regarding the full length of the 1906 rupture. Original investigations of surface rupture are summarized in Lawson (1908) and include a description of surface rupture as far north as Shelter Cove. Much later, McLaughlin et al. (1979, 1983) questioned these reports on the basis of bedrock mapping, which indicated that the main fault strand had not displaced features dated at ~13,000 years BP. Seismological evidence does not require slip on the San Andreas Fault north of Point Arena, though Thatcher et al. (1997) infer from geodetic data that ~8.6 m of slip occurred on the fault in the Shelter Cove area. Brown (1995) re-examined surface morphology and the original field reports by F.E. Mathes from 1906, and he concluded that the original reports of surface rupture were correct and that many effects of the rupture are still observable today. Most recently, Prentice et al. (1999) also re-examined Mathes' field notes and photographs and trenched along the 1906 rupture. Like Brown (1995), they conclude that abundant evidence for a 1906 rupture exists and estimate a minimum slip-rate

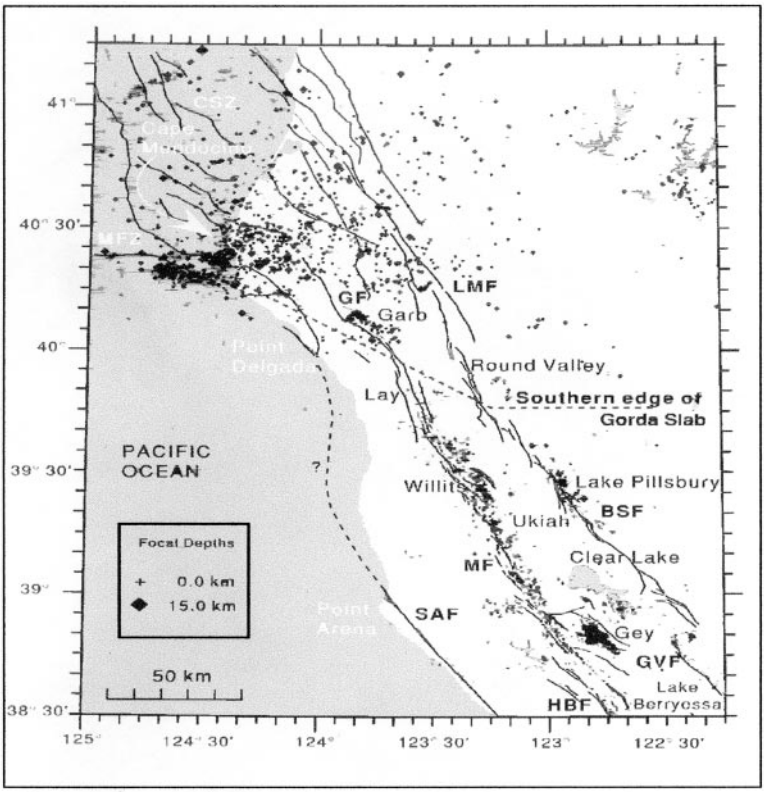

Figure 7 Major faults of northern California and seismicity > magnitude 1.5 for the time period 1980–1991. Dashed line is surface projection of the southern edge of the Gorda slab (Jachens & Griscom 1983). CSZ, Cascadia subduction zone; BSF, Bartlett Springs Fault; Garb, Garberville; GF, Garberville Fault; Gey, geysers; GFV, Green Valley Fault; HBF, Healdsburg Fault; Lay, Laytonville; LMF, Lake Mountain Fault; MF, Maacama Fault; MFZ, Mendecino Fracture Zone; and SAF, San Andreas Fault (figure from Castillo & Ellsworth 1993).

of 14 mm/year for the northern San Andreas Fault based on a 180-m offset of colluvial deposits dated at 13,180 ± 170 cal years BP. The southern end of the rupture extends as far south as the Santa Cruz mountains (Schwartz et al. 1998), giving a minimum rupture length of ∼470 km.

NORTHERN SAN ANDREAS ONSHORE PALEOSEISMICITY

The paleoseismology of the northern San Andreas Fault (summarized in Figure 8) has been investigated at Olema, 45-km north of San Francisco; at Dogtown, close to the Olema site; at Point Arena; and at Grizzly Flats in the Santa Cruz mountains. At

the Vendanta site near Olema, Niemi & Hall (1992) found that offset stream channels showed that the fault ruptured along a single main strand, and offset stream deposits dated at 1800 ± 78 years by 40–45 m. The maximum late-Holocene slip rate derived from these data is 24 ± 3 mm/year, in good agreement with geodetic data. They estimate that if the 4–5-m slip event recorded in 1906 were characteristic, the recurrence time for such events would be 221 ± 40 years. At Point Arena, 145 km to the northwest, Prentice (1989) recognized four events that offset a Holocene alluvial fan channel 64 ± 2 m. The maximum slip rate calculated at Point Arena is 25.5 mm/year, in excellent agreement with the Olema data. The average slip per event at Point Arena implies a recurrence time of 200–400 years (Prentice 1989). Dated offset terrace deposits suggest that this rate has not changed by more than approximately 20% since Pliocene time. The best age derived for the penultimate event is the mid-1600s (Schwartz et al. 1998), and the most likely ages for the previous three events were ~1300 (post AD 1150, pre AD 1650) for the third event, and two events pre–AD 1210 and post–AD 1, totaling five events in 2000 years (Prentice 1989, 2000; Niemi & Zhang 2000). Schwartz et al. (1998) also show an additional event at several sites in the early mid-1500s.

A controversial aspect of northern San Andreas Fault tectonics has been whether the fault is segmented, with variable behavior for each segment, or whether the 1906 earthquake, rupturing the entire northern San Andreas Fault from the creeping section in central California to the Mendocino triple junction, was characteristic. The consistent slip rates found north of the Golden Gate slow to approximately 17 mm/year south of the Golden Gate. This and a lower coseismic slip in 1906 south of the Golden Gate (Segall & Lisowski 1990, Thatcher et al. 1997, Prentice & Ponti 1997) led investigators to conclude that the fault is segmented near the Golden Gate. The Working Group on California Earthquake Potential (1990) applied a uniform slip rate to the fault and concluded that segments with lower coseismic slip in 1906 should have more frequent events to fill the slip deficit. Schwartz et al. (1998) argue that the segmentation is simply a consequence of the offshore San Gregorio Fault (Figure 8) absorbing some of the slip, and the slip-rate on the main San Andreas Fault is correspondingly reduced. They argue that the through-going rupture in 1906 is characteristic, and further, that the penultimate event, which occurred in the mid-1600s, ruptured approximately the same distance and magnitude as the 1906 event.

NEW RESULTS: NORTHERN SAN ANDREAS TURBIDITE RECORD

During our 1999 Cascadia cruise, we collected two piston cores and one box core from Noyo Channel 150-km south of the southern end of the Cascadia subduction zone. We found that the Noyo Channel cores near the offshore northern San Andreas fault contain a good cyclic record of turbidite beds (Figures 5 and 6). In Core 49PC, we found 31 turbidite beds above the Holocene/Pleistocene boundary.

Thus far, we have determined ages for 20 (of 38) events, including the uppermost 5 events from cores 49PC/TC and adjacent box core 50BC, using AMS methods. The record for the past 2000 years for both onshore and offshore sites is shown in Figure 8. The uppermost turbidite event returns a "modern" age, which we interpret is likely the 1906 San Andreas earthquake. The penultimate event returns an intercept age of AD 1663 (2σ range 1505–1822). The third and fourth events are lumped together, as there is no hemipelagic sediment between them. The age of this possible couplet event is AD 1524 (1445–1664). The fifth event age is AD 1204 (1057–1319), and the sixth event age is AD 1049 (981–1188). These results are in relatively good agreement with the onshore work to date, which indicates an age for the penultimate event in the mid-1600s (Figure 7), the most likely age for the third event is ~AD 1500–1600, and a fourth event ~AD 1300. We presently do not have the spatial sampling needed to test for synchroneity of events along the northern San Andreas Fault, and thus we cannot determine with confidence that the observed turbidite record is earthquake generated. However, the good agreement in number of events between the onshore and offshore records suggests either a coincidence or that turbidite triggers other than earthquakes appear not to have added significantly to the turbidite record along the northernmost San Andreas margin during the last ~2000 years.

With new dates on 20 events, we can begin to make some preliminary observations about the turbidite-event history offshore California. Figure 9 shows the age of the core with depth and shows a good AMS age record, with no reversing

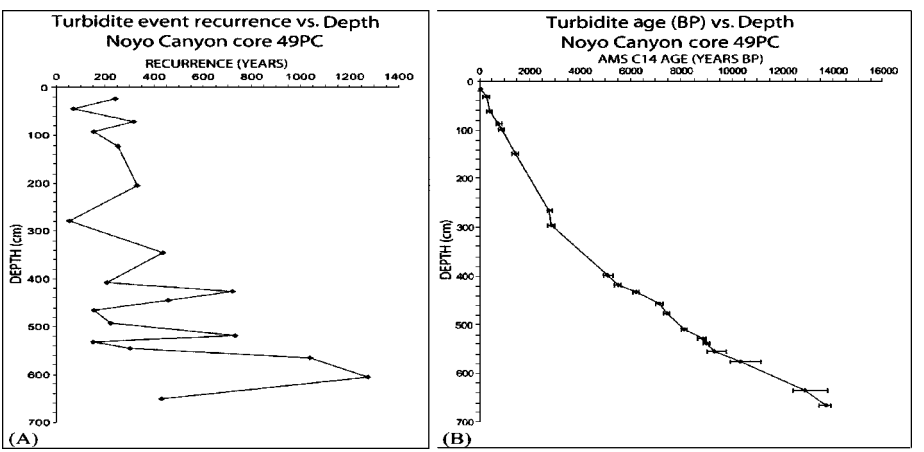

Figure 9 (*A*) Event recurrence versus core depth for Noyo Canyon core 49PC. (*B*) Event age versus depth in core 49PC. 2σ errors for *B* shown by horizontal bars. Both plots show an increase in the interval between events down-core. We cannot determine the origin of these rate changes with our single Noyo core. The youngest interval in *B* represents an average recurrence time of 216–234 years (events 3 and 4 could be either one or two events).

intervals in those dated so far. Figure 9*A* shows the recurrence interval of events plotted with depth. It is apparent from both plots that both sedimentation rate and turbidite-event frequency have not been constant through the Holocene. If the turbidite frequency is in fact an earthquake proxy, then the repeat time for events along the northernmost segment near Noyo Canyon has decreased with time during the Holocene. This may be due to a number of possible causes: (*a*) the behavior of the fault has changed, for example, more slip shifting from other parts of the plate boundary system to the main San Andreas Fault in the late Holocene; or (*b*) the record includes a nonearthquake climatic or sedimentation record that has changed through the Holocene. Climatic and sedimentation changes would tend to favor a reduction in sedimentation during the Holocene, as the sea level rose and separated canyons from their river sources, and terrestrial erosion rates fell. We observe just the opposite, with an increase in sedimentation rate that parallels the increase in turbidite frequency. This observation tends to support a change in fault behavior; however, this issue cannot be resolved with our single core. Systematic coring completed in 2002 may be able to resolve this major question through spatial and temporal correlations as it has in Cascadia.

DISCUSSION

As the Cascadia turbidite project has matured, we have learned a number of things about the subtleties of using turbidites to precisely date earthquakes. The most important is that regional and temporal correlations are the strongest evidence of earthquake triggering, and radiocarbon event ages are much less so. This is not surprising and is simply the result of the errors and unknowns inherent in this process. Some of these problems have been known to land paleoseismologists for years; others are unique to the deep-sea environment. Our goals in radiocarbon dating have not been to use the ages to demonstrate earthquake origins because the spatial and temporal correlations do a much better job of that. The purpose of the ages is to attempt a correlation with the land record and to begin to integrate the two to cull more information about the earthquakes themselves in terms of the spatial and temporal patterns of strain release, about which we presently know very little.

Correlating paleoseismic events using the calibrated ages has long been problematic in paleoseismology. Because the ages themselves include many sources of error that must be propagated, it is sometimes difficult to get even known events to correlate this way. Land paleoseismologists have worked to overcome this problem by using large quantities of ages to do statistical analyses of the “cloud” of data associated with each event, in order to make the correlation more robust. With offshore data, we are unable to use that tool at present because the expense of collecting the original samples with a large ship has thus far precluded collecting enough sample volume to obtain more than one or two dates from each event. The limitation is imposed by the abundance of the planktonic forams that we are dating,

of which there are just enough in one or two 4" diameter cores below each event for one or two ages. What we do have in the offshore record is a longer record at multiple locations. This provides another way to arrive at a robust record. As mentioned above, pattern matching offers a way to discern a robust signal with less dependence on the individual data points, which may be in error for a variety of reasons. With multiple plots of recurrence, turbidite thickness, hemipelagic thickness, velocity, magnetic susceptibility, etc., we can correlate events and do statistical analysis on the correlations. This, in turn, can then be used to identify outliers.

In Figure 3 we also show the land data from Willapa Bay (Atwater & Hemphill-Haley 1997), a record from Lagoon Creek in northern California (near the Klamath River, Garrison-Laney et al. 2002), Humboldt Bay (Clarke & Carver 1992), and southern Oregon (Kelsey et al. 2002). These records show similarities to the longer offshore record, but it is too early to comment extensively. Our first complete core shows differences with events T2 and T3 of the onshore record, which we suspect may be due to the proximal environment of core 12PC.

Previously, we and others have noted a discrepancy between the average recurrence time seen in the marsh record and the average recurrence time from the turbidite record. With a more complete set of records, we think that this apparent discrepancy may simply be an artifact of the different time spans being reported. Our average reported repeat time of ~600 years is for the 13 post-Mazama events. Now, with a complete record for one of our key cores, we see that if we calculate recurrence intervals for the same time span that Atwater et al. (1987) do, we get a very similar result. At Willapa Bay, Atwater & Hemphill-Haley (1997) report an average repeat time of 533 years (7 events in 3500 years); Kelsey et al. (2002) report 529 years for the Sixes River in Southern Oregon (11 events in 5500 years), and Garrison-Laney et al. (2002) report 608 years for Lagoon Creek. In our record for the youngest Holocene interval, we calculate an average recurrence of 490–550 years for the past 3500–4000 years. Consequently, it may be that at least for the past 3000–4000 years, there is no discrepancy, and thus it will be possible to correlate events one-for-one. This adds strength to both the land and offshore records, in that upper-plate events appear not to be significant. This is so at least for the data analyzed thus far for Washington, Oregon, and northern California as far south as Humboldt Bay, with an exception in southern Oregon sites where "extra" events are apparent in the land record.

The curves show a possible anomaly in the 3000–4000-year range between the records in southern Oregon, the coastal records to the north and south, and the turbidite record. As did Kelsey et al. (2002), we observe "extra" events in the onshore records from Bradley Lake and the Sixes River areas relative to both the onshore record and our turbidite record. Our Rogue cores directly sample the subduction zone at this latitude, and the record of turbidites matches the other offshore records. Apparently southern Oregon experiences earthquakes or some other phenomenon that leaves similar records, in addition to the regional great-earthquake record. These could be upper plate events, smaller interplate events, or may possibly have some other origin.

While turbid flows may be triggered by a number of natural causes, turbidites remain a viable earthquake proxy in tectonic settings that are geologically, sedimentologically, and physiographically favorable. Work in Cascadia, the Northern San Andreas, and Japan has shown that favorable factors include: (*a*) separation of rivers and canyons by distance, or longshore currents that effectively buffer hyperpycnal flow; (*b*) presence of channel confluences that can be used to test synchronicity, a powerful relative dating technique; (*c*) a sediment supply that is not too high or too low to result in self-triggered slides or absence of slides during an earthquake, respectively; (*d*) canyon heads that are deep enough not to be subject to storm waves; (*e*) channel systems that are large enough and long enough to accommodate large turbid flows that can travel long distances relative to more localized flows, thus filtering out "noise" from small local events.

CONCLUSIONS

Results from Cascadia thus far support the conclusion that 18 large earthquakes may have ruptured at least the northern 2/3 of the plate boundary that we have examined. Synchronous triggering of turbid flows in several Washington channels has now been demonstrated for 18 events spanning the entire Holocene. Radiocarbon ages cannot prove or disprove synchronicity for the 18 events observed in other channels. While segmented rupture with close temporal spacing cannot be ruled out, the identical records found in the Rogue channel would have to be produced by a remarkably consistent long-term rupture pattern, with essentially no variability through 18 events over 9850 years. We are also encouraged by the close agreement between preliminary data and the onshore paleoseismic record along the Northern San Andreas Fault. Preliminary results from Noyo Channel indicate the potential for applying this method, utilizing additional cores from other channels, to fully develop the Holocene event-history of the Northern San Andreas Fault system. Most importantly, by carefully correlating the turbidite and land records, it should be possible to construct reliable event records back ~10,000 years for Cascadia, the Northern San Andreas, and other fault systems. Doing so would allow investigations of clustering, triggering, and other recurrence models, which are presently difficult to test due to the relatively short instrumental, historical, and onshore-paleoseismic records.

ACKNOWLEDGMENTS

We thank the officers and crew of the Scripps Vessel R.V. Melville with special thanks to Bob Wilson. We thank the members of the Scientific Party: Drew Erickson, Mike Winkler, Pete Kalk, Julia Pastor, Antonio Camarero, Clara Morri, Gita Dunhill, Luis Ramos, Alex Raab, Nick Pisias Jr., Mark Pourmanoutscheri, David Van Rooij, Lawrence Amy, and Churn-Chi "Charles" Liu. This research was supported by National Science Foundation grants EAR-0001023, EAR-017120,

and EAR-9803081 and U.S. Geological Survey National Earthquake Hazards Reduction Program award 01HQGR0051, and Cooperative Agreement 1434WR97AG00016. We also thank Mary Lou Zoback for her thoughtful review that much improved the paper.

The *Annual Review of Earth and Planetary Science* is online at http://earth.annualreviews.org

LITERATURE CITED

Adams J. 1990. Paleoseismicity of the Cascadia subduction zone: evidence from turbidites off the Oregon-Washington margin. *Tectonics* 9:569–83

Anastasakis GC, Piper DJW. 1991. The character of seismo-turbidites in the S-1 sapropel, Zakinthos and Strofadhes basins, Greece. *Sedimentology* 38:717–33

Argus DF, Gordon RG. 1991. Current Sierra Nevada-North America motion from very long baseline interferometry: implications for the kinematics of the western United States. *Geology* 19:1085–19

Atwater BF. 1987. Evidence for great Holocene earthquakes along the outer coast of Washington State. *Science* 236:942–44

Atwater BF. 1992. Geologic evidence for earthquakes during the past 2000 years along the Copalis River, southern coastal Washington. *J. Geophys. Res.* 97:1901–19

Atwater BF, Hemphill-Haley E. 1997. *Recurrence intervals for great earthquakes of the past 3500 years at northeastern Willapa Bay, Washington. US Geol. Surv. Prof. Pap. 1576.* 108 p.

Atwater BF, Nelson AR, Clague JJ, Carver GA, Yamaguchi DK, et al. 1995. Summary of coastal geologic evidence for past great earthquakes at the Cascadia subduction zone. *Earthq. Spectra* 11:1–18

Brown RD. 1995. 1906 surface faulting on the San Andreas Fault near Point Delgada, California. *Bull. Seismol. Soc. Am.* 85(1)100–10

Castillo DA, Ellsworth WL. 1993. Seismotectonics of the San Andreas Fault System between Point Arena and Cape Mendocino in northern California: implications for the development and evolution of a young transform: *J. Geophys. Res.* 98:6543–60

Clague J, Atwater B, Wang K, Wand MM, Wong I, eds. 2000. *Proceedings of the GSA Penrose Conference Great Cascadia Earthquake Tricentennial*. Portland, OR: Oregon Dept. Geol. Miner. Ind. 156 pp.

Clarke SH, Carver GA. 1992. Breadth of interplate coupling in the southern Cascadia subduction zone: implication for earthquake magnitudes. *Geol. Soc. Am. Abstr. Progr.* 24:15

Darienzo ME, Peterson CD. 1990. Episodic tectonic subsidence of late Holocene salt marshes, northern Oregon central Cascadia margin. *Tectonics* 9:1–22

DeMets C, Dixon TH. 1999. New kinematic models for Pacific-North America motion from 3 Ma to present; I, evidence for steady motion and biases in the NUVEL-1A model. *Geophys. Res. Lett.* 26:1921–24

Field ME. 1984. The submarine landslide of 1980 off Northern California. *US Geol. Surv. Circ.* 938:65–72

Fumal T, Heingartner GF, Schwartz DP. 1999. Timing and slip of large earthquakes on the San Andreas Fault, Santa Cruz Mountains, California. *Geol. Soc. Am. Abstr. Progr.* 31:A–56

Garfield N, Rago TA, Schnebele KJ, Collins CA. 1994. Evidence of a turbidity current in Monterey submarine canyon associated with the 1989 Loma Prieta earthquake. *Cont. Shelf Res.* 14(6):673–86

Garrison-Laney CE, Abramson HF, Carver GA. 2002. Late Holocene tsunamis near the

southern end of the Cascadia subduction zone. *Seismol. Res. Lett.* 73(2):248

Goldfinger C, Nelson CH, Johnson JE. 1999. Holocene recurrence of Cascadia great earthquakes based on the turbidite event record. *EOS Trans. Am. Geophys. Union* 80:1024

Goldfinger C, Kulm LD, Yeats RS, Hummon C, Huftile GJ, et al. 1996. Oblique strike-slip faulting of the Cascadia submarine forearc: the Daisy Bank fault zone off central Oregon, subduction: top to bottom, Geophysical Monogr. 96, Am. Geophys. Union pp. 65–74

Gorsline DS, De Diego T, Nava-Sanchez EH. 2000. Seismically triggered turbidites in small margin basins: Alfonso Basin, Western Gulf of California and Santa Monica Basin, California Borderland. *Sediment. Geol.* 135:21–35

Grantz A, Phillips RL, Mullen MW, Starratt SW, Jones GA, et al. 1996. Character, paleoenvironment, rate of accumulation, and evidence for seismic triggering of Holocene turbidites, Canada abyssal plain, Arctic Ocean. *Mar. Geol.* 133:51–73

Griggs GB, Carey AG, Kulm LD. 1969. Deep-sea sedimentation and sediment-fauna interaction in Cascadia Channel and on Cascadia abyssal plain. *Deep-Sea Res.* 16:157–70

Griggs GB, Kulm LD. 1970. Sedimentation in Cascadia deep-sea channel. *Geol. Soc. Am. Bull.* 81:1361–84

Heezen BC, Ewing M. 1952. Turbidity currents and submarine slumps, and the 1929 Grand Banks earthquake. *Am. J. Sci.* 250:849–73

Hempill-Haley E. 1995. Diatom evidence for earthquake-induced subsidence and tsunami 300 yr age in southern coastal Washington. *Geol. Soc. Am. Bull.* 107:367–78

Hemphil-Haleyl E, Nelson AR, Kelsey HM, Witter RC. 2000. Displaced marine diatoms in a coastal fresh-water lake: microfossil evidence for Holocene tsunamis on the south-central Oregon coast. See Clague et al. 2000, p. 53

Hutchinson I, Clague JJ, Bobrowsky PT, Williams HFL. 2000. Investigations of Cascadia paleoseismicity in southwestern B.C. and northernmost Washington State. See Clague et al. 2000, p. 61

Inouchi Y, Kinugasa Y, Kumon F, Nakano S, Yasumatsu S, Shiki T. 1996. Turbidites as records of intense palaeoearthquakes in Lake Biwa, Japan. *Sediment. Geol.* 104:117–25

Jacoby GC, Bunker DE, Benson BE. 1997. Tree-ring evidence for an A.D. 1700 Cascadia earthquake in Washington and northern Oregon. *Geology* 25(11):999–1002

Jachens RC, Griscom A. 1983. Three-dimensional geometry of the Gorda plate beneath northern California. *J. Geophys. Res.* 88:9375–92

Karlin RC, Abella SEB. 1992. Paleoearthquakes in the Puget Sound region recorded in sediments from Lake Washington, U.S.A. *Science* 258:1617–20

Kastens KA. 1984. Earthquakes as a triggering mechanism for debris flows and turbidites on the Calabrian Ridge. *Mar. Geol.* 55:13–33

Kelsey HM, Witter RC, Hemphill-Haley E. 1998. Response of a small Oregon estuary to coseismic subsidence and postseismic uplift in the past 300 years. *Geology* 26(3):298–314

Kelsey HM, Witter RC, Hemphill-Haley E. 2002. Plate-boundary earthquakes and tsunamis of the past 5500 yr, Sixes River estuary, southern Oregon. *Geol. Soc. Am. Bull.* 114(3)298–314

Lawson AC. 1908. *The California earthquake of April 18, 1906.* Rep. State Earthq. Investig. Comm. Carnegie Institution, Washington, DC. Vols. I, II

MacKay ME, Moore GF, Cochrane GR, Moore JC, Kulm LD. 1992. Landward vergence and oblique structural trends in the Oregon margin accretionary prism: implications and effect on fluid flow. *Earth Planet. Sci. Lett.* 109:477–91

McLaughlin RJ, LaJoie KR, Sorg DH, Morrison SD, Wolfe JA. 1983. Tectonic uplift of a middle Wisconsin marine platform near the Mendocino triple junction, California. *Geology* 11:35–39

McLaughlin RJ, Sorg DH, Morton JL, Batchelder JN, Heropoulos HN, et al. 1979.

Timing of sulfide mineralization and elimination of the San Andreas fault at Point Delgada, California. *EOS Trans. Am. Geophys. Union* 60:883

Nakajima T, Kanai Y. 2000. Sedimentary features of seismoturbidites triggered by the 1983 and older historical earthquakes in the eastern margin of the Japan Sea. *Sediment. Geol.* 135:1–19

Nelson AR, Atwater BF, Brobowski PT, Bradley LA, Clague JJ, et al. 1995. Radiocarbon evidence for extensive plate-boundary rupture about 300 years ago at the Cascadia subduction zone. *Nature* 378:371–74

Nelson AR, Kelsey HM, Hemphill-Haley E, Witter RC. 2000. Oxcal analyses and varve-based sedimentation rates constrain the times of c14 dated tsunamis in southern Oregon. See Clague et al. 2000, pp. 71–72

Nelson H. 1976. Late Pleistocene and Holocene depositional trends, processes, and history of Astoria deep-sea fan, northeast Pacific *Mar. Geol.* 20:129–73

Nelson CH, Goldfinger C. 1999. Turbidite event stratigraphy and implications for Cascadia basin paleoseismicity. *EOS Trans. Am. Geophys. Union* 80:733

Nelson CH, Kulm LD, Carlson PR, Duncan JR. 1968. Mazama ash in the northeastern Pacific. Science 161:47–49

Nelson CH, Savoye B, Rehault JP, Escutia C. 1995a. *Interfingering of western Corsican margin aprons with the Var Fan lobe and an apparent Late Quaternary Corsican paleoseismic event*, Int. Assoc. Sediment. Region. Eur. Meet., 16th, Aix-les-Bains, Savoie, France, Abstracts Volume, p. 113

Niemi TM, Ben-Avraham Z. 1994. Evidence for Jericho earthquakes from slumped sediments of the Jordan River delta in the Dead Sea. *Geology* 22:395–98

Niemi TM, Hall NT. 1992. Late Holocene slip rate and recurrence of great earthquakes on the San Andreas fault in northern California. *Geology* 20:195–98

Niemi T, Zhang H. 2000. Paleoseismology of the northern San Andreas Fault at the Vendanta Marsh Site, Marin County, CA. 3rd Conference on Tectonic Problem of the San Andreas Fault System, Stanford, CA

Normark WR, Piper DJW. 1991. Initiation processes and flow evolution of turbidity currents: implications for the depositional record. In *From Shoreline to Abyss: Contributions in Marine Geology in Honor of Francis Parker Shepard, SEPM Spec. Publ. 46*, ed. RH Osborne, pp. 207–30. Tulsa, OK: Soc. Econ. Paleontol. Mineral.

Ollerhead J, Huntley DJ, Nelson AR, Kelsey HM. 2001. Optical dating of tsunami-laid sand from an Oregon coastal lake. *Quat. Sci. Rev.* 20(18):1915–26

Oppenheimer D, Beroza G, Carver G, Dengler L, Eaton J, et al. 1993. The Cape Mendocino California earthquakes of April 1992: subduction at the triple junction. *Science* 261:433–38

Pilkey OH. 1988. Basin plains; giant sedimentation events. *Geol. Soc. Am. Spec. Pap.* 229:93–99

Prentice CS. 1989. Earthquake geology of the Northern San Andreas Fault near Point Arena, California. PhD thesis. Calif. Inst. Technol., Pasedena, Calif. 252 p.

Prentice CS, Langridge R, Merritts D. 2000. Paleoseismic and Quaternary tectonic studies of the San Andreas Fault from Shelter Cove to Fort Ross. In *3rd Conference on Tectonic Problems of the San Andreas Fault System*, Stanford, CA

Prentice CS, Merritts DJ, Beutner EC, Bodin P, Schill A, Muller JR. 1999. Northern San Andreas fault near Shelter Cove, California. *Geol. Soc. Am. Bull.* 111:512–23

Prentice CS, Ponti DJ. 1997. Coseismic deformation of the Wrights tunnel during the 1906 San Francisco earthquake: a key to understanding 1906 fault slip and 1989 surface ruptures in the southern Santa Cruz Mountains, California. *J. Geophys. Res.* 102:635–48

Satake K, Shimazaki K, Tsuji Y, Ueda K. 1996. Time and size of a giant earthquake in Cascadia inferred from Japanese tsunami records of January, 1700. *Nature* 379:246–49

Schnellmann M, Anselmetti FS, Giardini D,

Ward SN. 2002. Prehistoric earthquake history revealed by lacustrine slump deposits. *Geology* 30:1131–34

Sauber JW, Thatcher W, Solomon SC, Lisowski M. 1994. Geodetic slip-rate for the eastern California shear zone and the recurrence time for Mojave desert earthquakes. *Nature* 367:264–66

Schwartz DP, Pantosti D, Okumura K, Powers TJ, Hamilton JC. 1998. Paleoseismic investigations in the Santa Cruz mountains, California: implications for recurrence of large-magnitude earthquakes on the San Andreas fault. *J. Geophys. Res.* 103(8):17985–8001

Schwartz DP, Working Group on California Earthquake Probabilities . 1999. *Earthquake probabilities in the San Francisco Bay region 2000–2030—A summary of findings*. *US Geol. Surv. Open File Rep. 99-517*. 56 pp.

Seely DR. 1977. The significance of landward vergence and oblique structural trends on trench inner slopes. In *Island Arcs, Deep Sea Trenches and Back-Arc Basins*, ed. M. Talwani, WC Pitman, Maurice Ewing Ser. I:187–98. Washington, DC: Am. Geophs. Union

Segall P, Lisowski M. 1990. Surface displacement in the 1906 and 1989 Loma Prieta earthquakes. *Science* 250:1241–44

Shiki T, Kumon F, Inouchi Y, Kontani Y, Sakamoto T, et al. 2000. Sedimentary features of the seismo-turbidites, Lake Biwa, Japan. *Sediment. Geol.* 135:37–50

Southon JR, Nelson DE, Vogel JS. 1990. A record of past ocean-atmosphere radiocarbon differences from the Northeast Pacific. *Paleoceanography* 5(2):197–206

Stein RS, King GCP, Jian L. 1992. Change in failure stress on the southern San Andreas fault system caused by the 1992 M 7.4 Landers earthquake. *Science* 199:1328–32

Sternberg RW. 1986. Transport and accumulation of river-derived sediment on the Washington continental shelf. *J. Geol. Soc. London.* 143:945–56

Stuvier M, Braziunas TF. 1993. Modeling atmospheric 14C influences and 14C ages of marine samples to 10,000 BC. *Radiocarbon* 35:137–89

Sugiyama Y. 1994. Neotectonics of Southwest Japan due to the right-oblique subduction of the Philippine Sea Plate. *Geofisica Int.* 33:53–76

Thatcher W, Marshall G, Lisowski M. 1997. Resolution of fault slip along the 470 km long rupture of the great 1906 San Francisco earthquake. *J. Geophys. Res.* 102:5353–67

Thomson J, Weaver PPE. 1994. An AMS radiocarbon method to determine the emplacement time of recent deep-sea turbidites. *Sediment. Geol.* 89:1–7

Ward SN, Goes SDB. 1993. How regularly do earthquakes recur? A synthetic seismicity model for the San Andreas fault. *Geophys. Res. Lett.* 20(19)2131–34

Westbrook GK. 1994. Growth of accretionary wedges off Vancouver Island and Oregon. *Proc. Ocean Drill. Prog., Initial Rep*. 146: (Pt. 1)381–88

Working Group on Northern California Earthquake Potential. 1990. *Probabilities of large earthquakes in the San Francisco Bay Region, California*. *US Geol. Surv. Circ. 1053*. 53 p.

Yamaguchi DK, Atwater BF, Bunker DE, Benson BE, Reid MS. 1997. Tree-ring dating the 1700 Cascadia earthquake. *Nature* 389:922–23

Zdanowicz CM, Zielinski GA, Germani MS. 1999. Mount Mazama eruption: calendrical age verified and atmospheric impact assessed. *Geology* 27:621–24

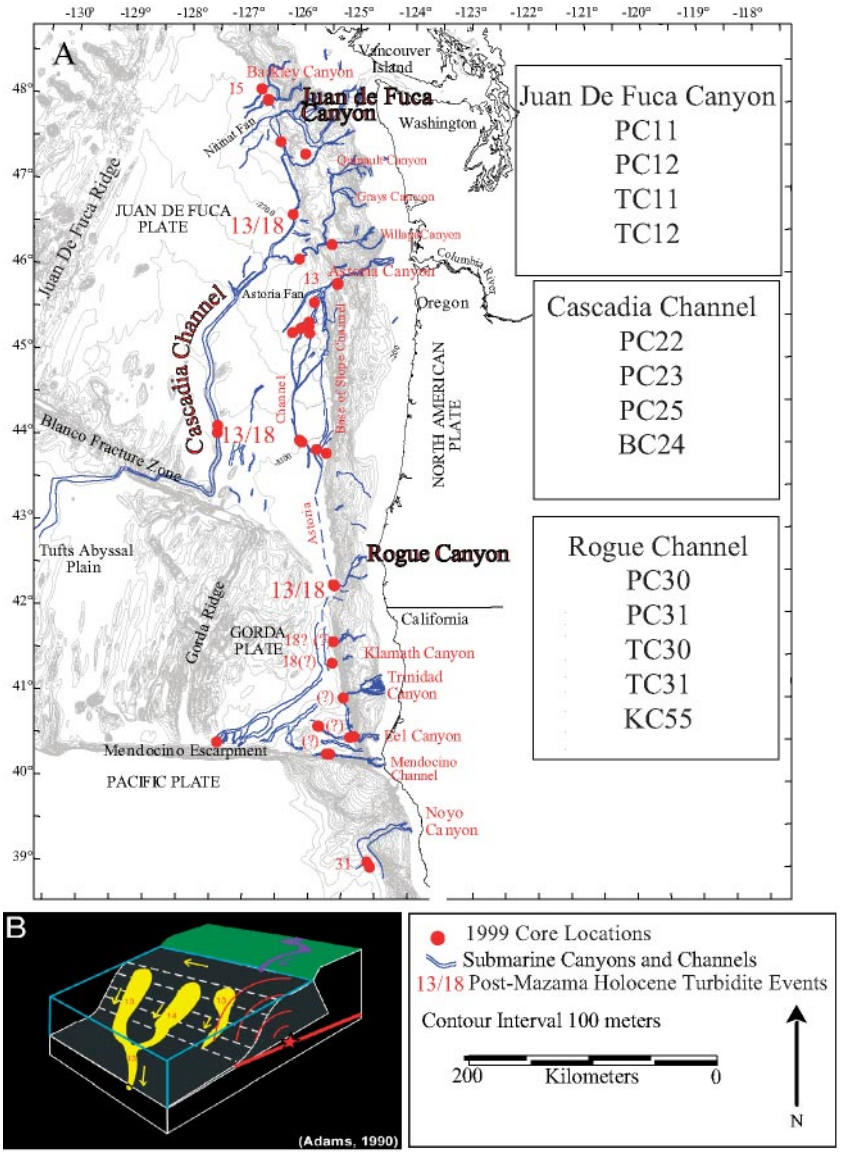

Figure 1 (*A*) Cascadia margin turbidite canyons, channels, and 1999 core locations. Major canyon systems and the number of post-Mazama and/or Holocene turbidites are shown next to core sites. Mazama ash was not present in Barkley Canyon cores or in the cores south of Rogue Canyon. Remarkable similarity of records in Cascadia suggests a central segment with a minimum of 600-km length. (*B*) Synchroneity test at a channel confluence as applied where Washington channels merge into the Cascadia Deep Sea Channel. The number of events below the confluence should be the sum of events in the tributaries, unless the turbidity currents were triggered simultaneously by an earthquake or other event.

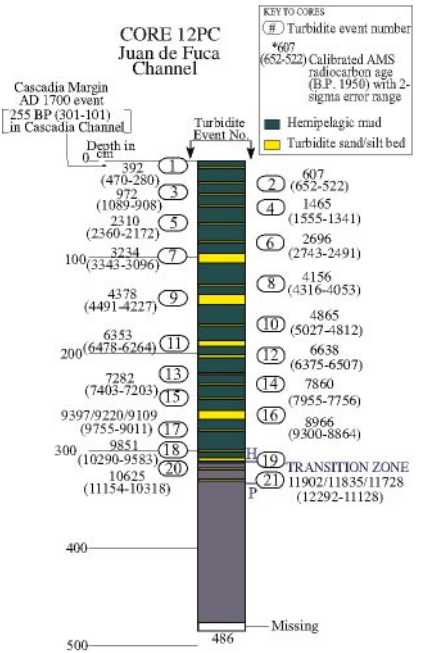

Figure 2 Schematic core diagram for piston core 12PC from Juan de Fuca Channel. Calibrated radiocarbon ages are shown with 2 sigma error ranges. Recurrence intervals between events are calculated and plotted in Figure 4.

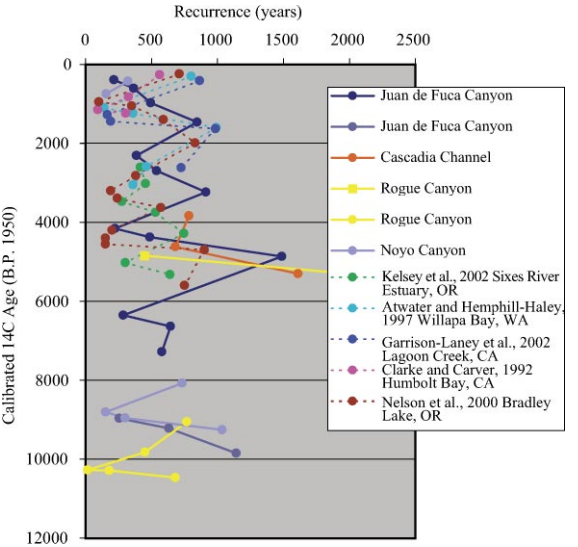

Figure 4 Summary of offshore and onshore calibrated 14C ages and recurrence intervals. Partial results from the turbidite record based on available radiocarbon ages. Note good agreement between Juan de Fuca Canyon and onshore records at 0–6000 years BP. "Extra" events in southern Oregon are indicated in the 3000–4000 BP range (also noted by Kelsey et al. 2002). For turbidite dates, intercept ages are shown; see Figure 2 for error ranges.

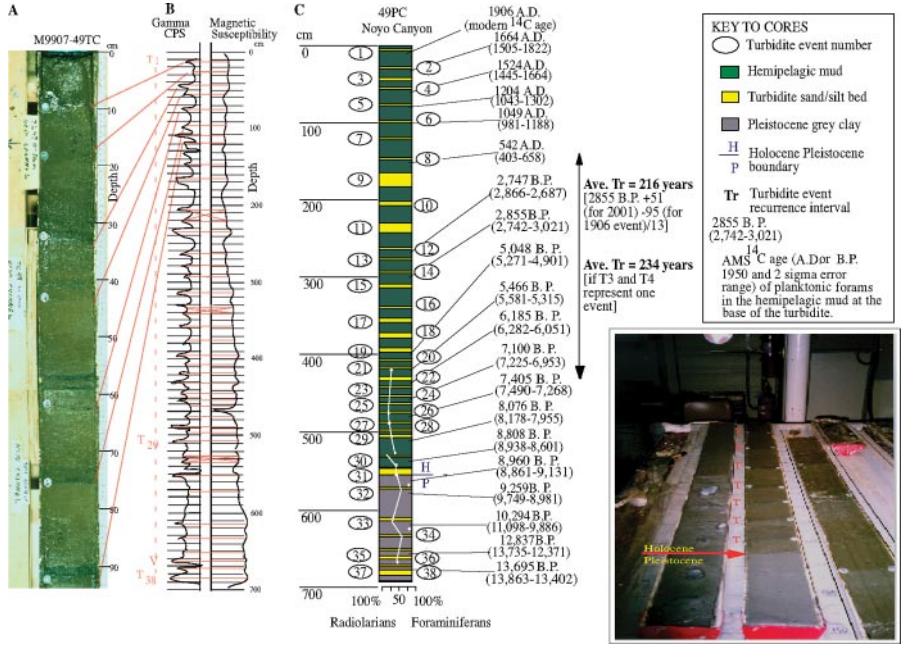

Figure 5 Top 93 cm of trigger core M9907-49TC (*A*) and the density and magnetic susceptibility logs (uncorrected) for the entire length (700 cm) of piston core M9907-49PC (*B*) from Noyo Canyon. Low density and high magnetic susceptibility identify and are used to correlate the turbidite events observed in the cores. Diagram of piston core (49PC) (*C*) is also shown. White buttons on the trigger core and the red horizontal lines on the log identify turbidite events. Average recurrence times (*C*) of 216 and 234 years are calculated based on the age of T14 and the 1906 event. The Holocene-Pleistocene boundary is defined here as the 1 to 1 ratio of radiolarians to forams (Duncan et al. 1970) (base of T31) and is shown as a white curve near the bottom of the core (*C*). **Figure 6** (*inset*) Sample core showing the sharp color change from light grey to olive-green, characteristic of the Pleistocene-Holocene boundary, and several thin, grey turbidite sands (labeled with Ts) separated by olive-green hemipelagic mud.

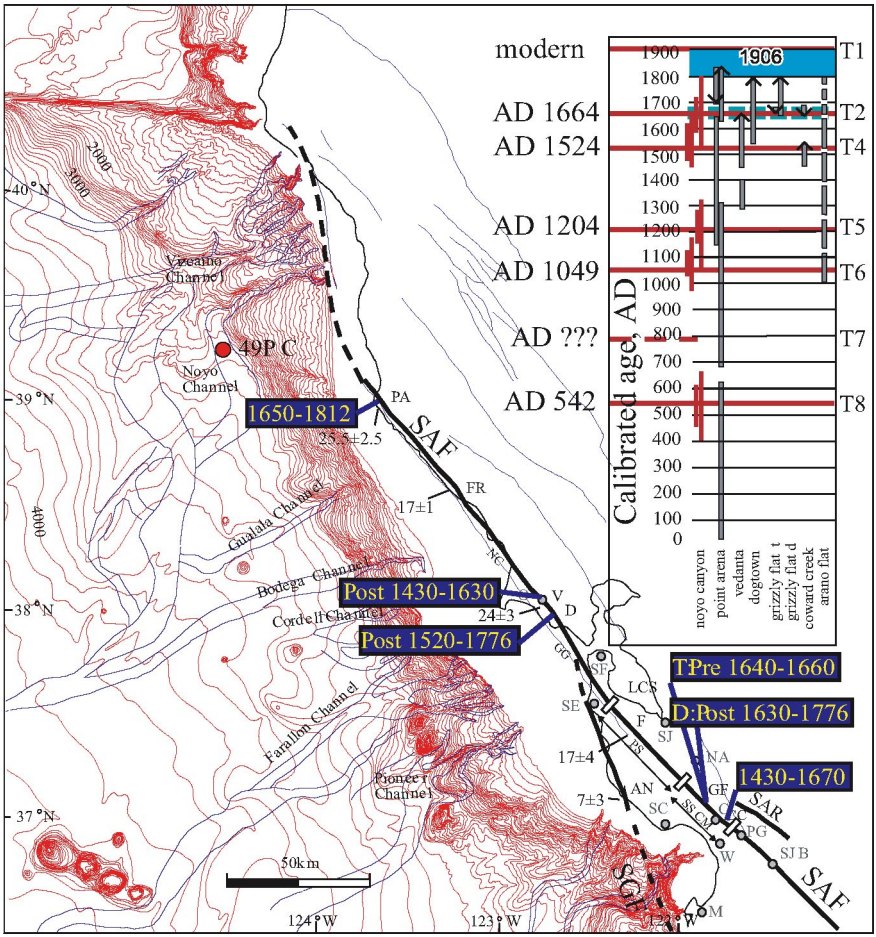

Figure 8 Most recent turbidite events and paleoseismic earthquakes on the Northern San Andreas Fault from 1999 core 49PC and onshore paleoseismic data. Inset shows age constraints for recent events reported at land sites with turbidite event data (T-values and horizontal red lines—because of erosion T3 cannot be dated). Horizontal dashed band in mid 1600s is the estimated age of the penultimate event from trenching (T) and dendrochronology (D) at Grizzly Flat. Grey vertical bars in inset show the 2 sigma age ranges of radiocarbon samples used to constrain the age of onshore recent events. Up arrows indicate the event postdates the age range; down arrows indicate the event predates the age range. Red vertical bars on turbidite events represent the one and two sigma range for Noyo Canyon ages. Numbers (with errors) and letters locate slip rates and event chronology sites. PA, Point Arena; FR, Fort Ross; V, Vedanta; O, Olema; D, Dogtown; GG, Golden Gate; SF, San Francisco; SE, Seal Cove; LCS, Lower Crystal Springs; F, Filoli; AN, Ano Nuevo; SJ, San Jose; NA, New Almaden; GF, Grizzly Flat; C, Corralitos; CC, Coward Creek; W, Watsonville; PG, Pajaro Gap; SJB, San Juan Bautista; SC, Santa Cruz; M, Monterey; NC, North Coast segment containing all segments. (Land data after Schwartz et al. 1998, modified from Niemi et al. 2000. Data added at Arano Flat from Fumal et al. 1999).